

# **COUPLED FLOW-THERMAL SCALABLE PROCESS MODELING SIMULATIONS IN LIQUID COMPOSITE MOLDING OF COMPOSITE STRUCTURES**

**Ram Mohan**

Center for Advanced Materials and Smart Structures  
Department of Mechanical Engineering  
North Carolina A&T State University  
Greensboro, NC 27411

## **ABSTRACT**

Net-shape liquid composite molding (LCM) processes for the manufacturing of composite structures involve the permeation of a reactive thermoset polymeric resin through complex, fiber woven preforms. The physical behavior during the processing thus involves coupled multi-physics phenomena consisting of mass, thermal and species transport. The flow process models based on conservation of mass are solved using conventional Galerkin finite element formulations coupled with an implicit fully transient pure finite element methodology. The convective nature of the thermal transport models however require the use of Stabilized Upwinding Petrov-Galerkin formulations and Peclet number controlled stable thermal time steps. In thin shell aerospace composite configurations, the process flow behavior is analyzed through 2.5D thin shell models, with an in-plane flow field that is volume averaged across the thickness (2D in-plane flow). The through thickness conduction however is predominant in the thermal models and cannot be neglected. Discussions on the scalable computational developments and modeling techniques for the coupled 2D-flow/3D-thermal analysis, verifications and validations are presented. The paper also discusses high end computing scalable simulation developments, implementations, issues, and performance of the coupled flow thermal process modeling and simulations in liquid composite molding processes for composite structures employing 2D-Flow/3D-Thermal model configurations.

## **INTRODUCTION**

Polymer based composite materials are increasingly used in aerospace and space structures. In aerospace and rotary wing structure applications, these tend to be load bearing, large-scale unitized structures. The manufacture of unitized aerospace structural composite materials poses significant problems. The strength of these composite material structures is due to the directional orientation of the individual fabric layers. Manufacturing techniques should ideally preserve this fiber orientation during processing, and with repeatability. Manufacturing techniques based on liquid composite molding (LCM) have evolved over the past decade to provide a production oriented methodology for structural composite configurations. This manufacturing process allows for repeated production of net-shape, load bearing composite structures that maintain and preserve the desired fiber lay-up orientation in a production environment. One particular type of LCM process used in the manufacture of aerospace structures is resin transfer molding (RTM) and its related variants. The process involves few steps starting with a mold or a tool cavity that could be one- or two- sided. This is followed by setting up a dry fiber preform with multiple layers of dry woven fabric (normally stitched together) and preforming the dry fabric into a net-shape of the composite structural configuration to be manufactured. The net-shape composite preform configuration is placed inside the mold cavity conforming to the tool surface. The reactive polymer resin is then injected into the mold cavity where it infiltrates and impregnates the dry fiber preform, followed by the consolidation into the net-shape composite structural configuration.

Integrated development of composite material structural configurations requires an understanding of the physical phenomena during the processing and the associated effect of the induced residual stresses that arise during the processing. The LCM process involves the permeation of the reactive thermoset polymeric resin through complex, fiber woven preforms. The physical behavior during the processing involves coupled multi-physics phenomena consisting of mass, thermal, and species transport. The physical and geometric complexity of the process requires coupled multi-physics computational models that need scalable, high performance computing resources. In the case of aerospace composite structures the thickness is small compared to the lateral dimensions of the part. Hence, process flow models are generally based on a volume averaged velocity field in the thickness directions. The

process flow modeling and simulations are thus based on two-dimensional thin shell element configurations of the composite part based on a 2D in-plane flow field that is volume averaged across the thickness. The thermal conduction in the thickness direction during the coupled thermal transport that exists during the flow and subsequent consolidation cannot be neglected. The thermal models thus require full 3D models that account for the through thickness conduction based on the underlying 2D thin shell models that are used for the flow analysis. This paper focuses on the computational developments, modeling techniques and tightly coupled flow-thermal scalable software developments for the coupled flow-thermal simulations in LCM.

In this paper, the physical models and computational methodologies for the flow and thermal process behavior are briefly discussed. Computational developments and issues in numerical development of 3D thermal model configurations from 2D thin shell flow process finite element models are discussed. An illustrative validation of the 2D-flow and 3D-thermal, scalable parallel developments with available experimental data and prior simulation results for the coupled model is presented. Implementation issues and performance of scalable coupled flow-thermal simulations are also briefly discussed.

## PHYSICAL PROCESS MODELING IN LCM

The LCM physical process models involve the analysis of the underlying mass, thermal and species conservation. The physical conservation model equations for the flow and thermal conservation in LCM processes is briefly described next.

### PROCESS FLOW MODELING

Resin mass conservation and process flow behavior models address the macroscopic transient resin flow infiltration through a complex fiber preform. A transient mass conservation equation coupled with the Darcian flow behavior (momentum conservation) in conjunction with a pure finite element methodology is used for tracking the resin progression inside a complex mold cavity representing the net-shape composite structural part. The transient mass conservation equation<sup>1</sup> is given by

$$\frac{d}{dt} \int_{\Omega} \Psi d\Omega = \int_{\Omega} \nabla \cdot \left( \frac{\bar{K}}{\mu} \nabla P \right) d\Omega \quad (1)$$

where,  $\bar{K}$  is the permeability tensor,  $\mu$  is the resin viscosity,  $P$  is the pressure field,  $\Psi$  is a state variable representing the infused state of the resin. The permeability tensor is a matrix of order two in most aerospace structures made of thin composite preform layers, where the flow velocity is primarily in the in-plane directions (2.5D physics). This flow process model based on conservation of resin mass is solved using conventional Galerkin finite element formulations coupled with an implicit fully transient pure finite element methodology for tracking the progressing flow front based on an Eulerian mesh for the mold cavity. This is briefly described next.

### Pure finite element methodology

The pure finite element methodology<sup>1</sup> is based on the above transient mass conservation equation for the tracking of the moving resin front boundary that can present several multiple as well as diverging and converging fronts.. The state variable  $\Psi$  ( $0 \leq \Psi \leq 1$ ) represents the infused state of a region.  $\Psi = 0$ , represents the un-infused regions of the dry fiber preform during the transient flow.  $\Psi = 1$ , represents the fully infused regions of the dry fiber preform. Applying Galerkin weighted residual formulation to the transient mass conservation equation, and introducing the finite element approximations for both the state variable  $\Psi$ , and the pressure field  $P$ , leads to a discretized system of equations given by

$$C\dot{\Psi} + KP = q \quad (2)$$

In the above equation,  $C$  is the mass matrix representing the pore volume,  $K$  is the stiffness matrix associated with the pressure field. The time derivative term is discretized using

$$\dot{\Psi} = \frac{\Psi_{n+1} - \Psi_n}{\Delta t} \quad (3)$$

where  $\Delta t$  is the time step size for the transient problem, and  $q$  is the force vector representing the injection conditions. The boundary conditions are given by

$$\begin{aligned} \frac{\partial P}{\partial n} &= \mathbf{0} \text{ on mold walls,} \\ P &= \mathbf{0} \text{ at flow front, and} \\ P &= P_0 \text{ prescribed pressure at inlet} \end{aligned} \quad (4)$$

$$\begin{aligned} &\text{or} \\ q &= q_0 \text{ prescribed flow rate at inlet,} \end{aligned}$$

where  $P_0$  and  $q_0$  represent prescribed pressure and flow rate at the inlet(s), respectively. Initially, at time  $t=0$ ,

$$\begin{aligned} \Psi &= \mathbf{1} \text{ at the inlet and} \\ \Psi &= \mathbf{0} \text{ elsewhere.} \end{aligned} \quad (5)$$

This methodology solves for the state variable defining the infusion state and the associated pressure field iteratively until a complete mass conservation is achieved at each step.

The pure finite element methodology briefly described here does not involve the restrictions of the time step increments seen in the explicit finite element-control volume<sup>2,3</sup> approach for the transient flow progression in this free surface flow problem (due to Courant stability considerations of the quasi-steady state approach). The methodology is second order accurate in time. It computes the transient flow behavior and position of the resin infusion front at each of the discrete time steps selected by the analyst. This leads to significant reductions in the computing time required for the process flow modeling and simulations in geometrically large composite aerospace structures. The computational advantage demonstrated by this method<sup>1</sup> in comparison to the explicit finite element-control volume technique for process flow modeling simulations in LCM is solely due to the computational methodology and the algorithmic solution strategy. This computational effectiveness is independent of the computing platform. Large scale process modeling and simulations for several aerospace structural configurations that were once impossible even in multi-processor scalable systems are now feasible with this methodology.

## THERMAL TRANSPORT MODELING

The thermal transient behavior during the process due to the heated resin systems and the exothermic curing reactions cannot be neglected during the resin flow infusion. This is further complicated by the changes in viscosity due to the change in temperature and degree of cure. The thermoset resin systems also begin to gel with the increase in degree of cure. The details of the thermal transport model equations, finite element discretizations following reference 6, are presented next.

### Thermal Transport Model

The thermal transport equations can either be based on two phase models or a local thermal equilibrium model. In the two phase model, the energy conservation equations for the resin and the fiber preform are written separately with the heat exchange between the two medium taken into account. As discussed in literature, the determination of this heat transfer coefficient that is different for each resin and fiber system and depends on the resin flow rate, and is quite cumbersome.<sup>4, 5, 6</sup>

In the present coupled flow thermal process modeling and simulation developments, the fiber and resin in the infused regions are assumed to be in local thermal equilibrium. The temperature of the resin and the fiber is the

same at any physical location infused with the resin. This is valid when the heat transfer coefficient between the resin and the fiber is large and the resin flow is slow<sup>4, 6</sup>, which is the case in most liquid composite molding processes. The local thermal equilibrium transport model is given by

$$\rho c_p \frac{\partial T}{\partial t} + \rho_r c_{pr} (u \cdot \nabla T) = \nabla \cdot k \nabla T + \phi \dot{G} \quad (6)$$

where  $\phi$  is the porosity of the fiber preform. The density  $\rho$ , specific heat capacity  $c_p$ , and the conductivity tensor  $k$  are weighted average values of these properties for the resin and fiber. This is given by

$$\begin{aligned} \rho c_p &= \phi \rho_r c_{pr} + (1 - \phi) \rho_f c_{pf} \\ k &= \phi k_r + (1 - \phi) k_f \end{aligned} \quad (7)$$

The conductivity term can also include thermal dissipation conductivity<sup>6, 7</sup> which is difficult to determine and is generally neglected in most cases. The convective term in the thermal transport equation is due to the resin flow and only involves properties corresponding to the resin.  $\dot{G}$  is the rate of heat generation from the cure reaction as well from other sources. The initial and boundary conditions for the thermal equilibrium equation are given by

$$\begin{aligned} \text{At mold wall:} & \quad T = T_w \\ \text{At mold inlet:} & \quad T = T_{r0} \text{ during filling} \\ \text{At resin front:} & \quad k \frac{\partial T}{\partial n} = (1 - \phi) \rho_r c_{pr} u \cdot n (T_{f0} - T) \\ \text{Initially at time } t=0: & \quad T(t=0) = T_w \end{aligned} \quad (8)$$

Where  $T_w$  is the mold wall temperature,  $T_{r0}$  is the initial resin temperature, and  $T_{f0}$  is the initial fiber temperature. The condition at the flow front interface is an energy balance within an infinitesimal volume including the interface. The energy acquired in the flow front is balanced by the heat into this volume. The adiabatic condition is imposed on the other side of the boundary where the flow has not yet reached<sup>4</sup>.

### Finite Element Discretization of Thermal Transport

The convective nature of the thermal transport equation requires the use of stabilization techniques through streamline up-winding Petrov-Galerkin formulations.<sup>8, 9</sup> The finite element discretizations are discussed next.

The introduction of the Petrov-Galerkin formulation in the thermal transport equilibrium equation (6) and invoking the Gauss-Green theorem yields

$$\begin{aligned} \int_{\Omega} W \rho c_p \frac{\partial T}{\partial t} d\Omega + \int_{\Omega} W \rho_r c_{pr} (u \cdot \nabla T) d\Omega - \int_{\Gamma} W (k \nabla T \cdot n) d\Gamma \\ + \int_{\Omega} \nabla W \cdot k \nabla T d\Omega - \int_{\Omega} W \phi \dot{G} d\Omega = 0 \end{aligned} \quad (9)$$

The Petrov-Galerkin weight function is denoted by  $W_i$ , and finite element shape functions by  $N_i$  for the nodal temperature values. The boundary thermal flux term is given by

$$k \nabla T \cdot n = -q \cdot n \quad (10)$$

The finite element discrete equation (9) reduces to

$$\begin{aligned}
& \left[ \int_{\Omega} W_i \rho c N_j d\Omega \right] \frac{\partial T}{\partial t} + \left[ \int_{\Omega} W_i \rho c (u \cdot \nabla N_j) d\Omega \right] T_j + \left[ \int_{\Omega} \nabla W_i k \nabla N_j d\Omega \right] T_j \\
& = \int_{\Gamma} W_i (-q \cdot n) d\Gamma + \int_{\Omega} W_i \phi \dot{G} d\Omega
\end{aligned} \tag{11}$$

The discretized system of equations can then be written as

$$C\dot{T} + (K_{ad} + K_{cond})T = Q_q + Q_G \tag{12}$$

The various terms in the above equation are defined by

$$\begin{aligned}
C &= \int_{\Omega} W^r \rho c N d\Omega \\
K_{ad} &= \int_{\Omega} W^r \rho c (u \cdot B_N) d\Omega \\
K_{cond} &= \int_{\Omega} B_w^r k B_N \\
Q_q &= \int_{\Gamma} W^r (-q \cdot n) d\Gamma \\
Q_G &= \int_{\Omega} W^r \phi \dot{G} d\Omega
\end{aligned} \tag{13}$$

$B_w$  is the spatial derivative of the weighting function,  $W$ , and  $B_N$  is the spatial derivative of the shape function  $N$ .

#### Stabilization via Streamline Upwinding Petrov Galerkin Method

The highly advection nature of the thermal energy transport in resin transfer molding simulations require stabilization of the numerical solutions to avoid the oscillations seen in such problems invoking traditional Galerkin approaches. The standard technique used with such advection problems is the use of some type of upwinding. This causes the coefficients in the discretized problem to be heavily weighted in the up-stream direction. This is achieved through in the finite element discretization through Petrov-Galerkin formulation where the weighting function is not identically equal to the shape function. The streamline upwinding Petrov-Galerkin shape functions used in the thermal transport equations is briefly discussed next.

The streamline upwinding Petrov-Galerkin method proposed by Brooks and Hughes<sup>9</sup> adds a perturbation to the standard Galerkin shape function. This addition minimizes the crosswind diffusion by directing the artificial diffusion tensor along the flow stream lines. The perturbed weighting function should be applied to all the terms in the thermal transport equation to minimize the artificial diffusion effects. The Petrov-Galerkin weighting function is defined as

$$W_i = N_i + p_i \tag{14}$$

where  $N_i$  is the standard Galerkin weighting functions that are continuous across the element boundaries and  $p_i$  are perturbation functions that are discontinuous across the inter-element boundaries. The perturbation  $p_i$  is defined as

$$p_i = \lambda (u \cdot \nabla N_i) \tag{15}$$

The coefficient  $\lambda$  is given by

$$\lambda = \zeta Cr \frac{h_e}{2|u|} \tag{16}$$

The terms in the equation 16 are given by

$$\zeta = \text{Coth}(Pe) - \frac{1}{Pe}$$

$$Pe = \text{Mesh Peclet Number} = \frac{\rho c_p |u| h_e}{k}$$

$u$  = average element velocity

$|u|$  = magnitude of velocity vector

$h_e$  = element characteristic length

$$Cr = \text{element Courant number} = \begin{cases} 1, & \text{for steady state problems} \\ \frac{|u|\Delta t}{h_e}, & \text{for transient problems} \end{cases}$$

### Thermal Time Discretization

In addition to the time step increment via the implicit pure finite element method for the flow problem discussed earlier, the semi-discrete equations for the thermal problem as discussed earlier have to be solved for each flow time step. The advective nature of the thermal transport equations requires the use of thermal stability controlled time steps based on the Peclet number. A sub-time stepping strategy in which each flow time step is sub-divided into several time steps based on the thermal stability considerations. The discussions on the thermal time discretization and the sub-time stepping strategy are presented next.

The commonly used method for solving the semi-discrete thermal transport equation given by equation (12) is the trapezoidal  $\theta$  family of methods. This method uses weighted average of the time derivative at two consecutive time steps. Following the discussions in reference 6, the temperature solution at time step  $(n+1)$  is given by

$$\hat{K}_{n+1} T_{n+1} = \hat{K}_n T_n + \hat{F}_{n,n+1} \quad (17)$$

where,  $K = K_{ad} + K_{cond}$ ;  $F = Q_q + Q_{\dot{c}}$ , as defined in equation 17.

$$\begin{aligned} \hat{K}_{n+1} &= C + K_{n+1} \theta \Delta t \\ \hat{K}_n &= C - K_n (1 - \theta) \Delta t \\ \hat{F}_{n,n+1} &= \Delta t_{n+1} [(1 - \theta) F_n + \theta F_{n+1}] \end{aligned} \quad (18)$$

The value of  $\theta$  defines four well known numerical time integration schemes. The value of  $\theta = 0$  corresponds to conditionally stable, first order accurate forward Euler; the value of  $\theta = 1/2$  corresponds to second order accurate, unconditionally stable Crank-Nicolson; the value of  $\theta = 2/3$  is unconditionally stable, first order accurate Galerkin method;  $\theta = 1$  is unconditionally stable; first order accurate backward Euler method. The sub-time stepping strategy employed for the thermal transport is presented next.<sup>6</sup>

### Sub-Time Stepping Strategy for Thermal and Species Transport

As discussed earlier, the flow transport equations march forward with a time step size that is defined by the user based on the size of the model and the resolution desired in the flow front. The temperature time step on the other hand is restricted by the mesh Peclet number and the Courant criterion. A Courant number of less than one is needed to ensure the stability of the thermal and cure solution. The fill time based on the pure implicit formulation is much larger than the stable temperature and cure time step. A multiple sub-time stepping approach is used. At each fill time step increment, the critical time step for each element based on the Courant stability condition is determined. The smallest of all these critical time steps gives the equivalent time step that is used to determine the sub-time steps for the thermal and cure problem. The thermal critical time step is smaller than or equal to the equivalent time step and is set to be an integer fraction of the flow time step.<sup>6</sup>

## COUPLED FLOW-THERMAL SCALABLE IMPLEMENTATIONS

As seen from the theoretical discussions of the physical process models and the numerical methodologies, the scalable software developments require a structured software development framework. The discretized linear system of equations that form the core of the non-isothermal scalable software developments require the use of optimal solvers based on the symmetric or un-symmetric nature of the linear system. While the linear systems for the flow process models are symmetric, the thermal and species transport equations are non-symmetric when the convective terms are involved. Several linear system solver libraries with applications to scalable computer systems such as PETSc, PSPACEs, etc., have been developed over the years for the solution of such linear systems<sup>10, 11</sup>. The numerical computations also require the use of basic linear algebra routines and matrix operations that can be effectively integrated using the library packages such as BLAS and LAPACK. In addition, the scalable software developments also have to be integrated with the graphical libraries and graphical user interfaces for pre- and post-processing. Brief discussions of scalable software implementations are discussed next.

As discussed earlier, the interdependent nature of the physical model variables and the use of several external libraries for the solution of linear system of equations, graphical user interfaces, and other related libraries, the scalable software developments are based on an object-oriented design framework. The interdependencies across the physical variables in the process that adds complexity to the non-isothermal scalable computations are shown in Figure 1. The scalable software implementations have evolved over the years from the serial versions,<sup>1,6</sup> and Fortran 90 and MPI versions of resin flow infusion<sup>12, 13, 14, 15</sup> with the addition of thermal and species transport. The scalable implementations build upon the developments and are now based on the Simple Object Oriented Computing Environment for the Finite Element Method (SPOOCFEM)<sup>16</sup>. This object oriented framework reduces the development time for scientific software development, promotes code growth and maturation and improves the code coupling capabilities. The scalable software implementation adopts several technologies for the coupled flow-thermal process modeling computations of transport phenomena in resin transfer molding. The scalable non-isothermal computations are based on nodal composition of the full problem domain into multiple sub-domains with non-overlapping nodes of the domains assigned to each one of the processors. The domain decomposition of the computational domain into sub-domains is obtained using graph partitioning techniques using available software such as Metis and ParMetis<sup>17, 18</sup>. The interface elements share nodes that are common to more than one processor. This permits the direct use of parallel versions of the linear solver routine library routines from PETSc and PSPACEs. Earlier implementations based on elemental decompositions required the use of our own multi-processor solvers based on iterative algorithms such as pre-conditioned conjugate gradient methods<sup>12</sup>.

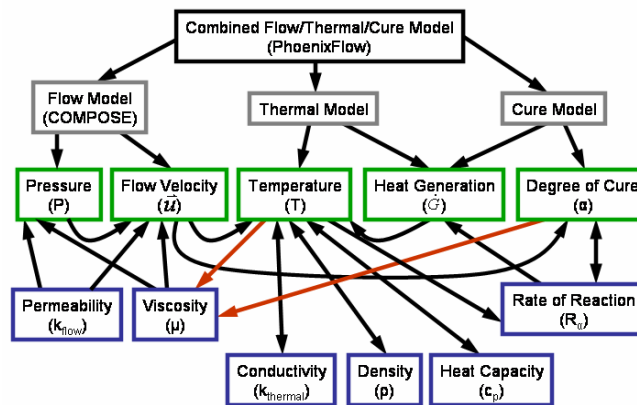


**Figure 1: Interdependencies of Problem Variables in Coupled Flow-Thermal Simulations**

## 2D-FLOW/3D-THERMAL MODELS FOR COUPLED FLOW-THERMAL COMPUTATIONS

In the case of thin shell composite configurations, the flow process models are based on thin shell finite elements with the associated thickness averaged in-plane flow velocity field. The thermal conduction in the through thickness directions cannot be neglected. To account for this through thickness thermal conduction, the thermal three-dimensional elements are built from the original two dimensional shell element configurations<sup>6</sup> as shown in figure 2. This does not require physically creating the three-dimensional model configurations for the thermal analysis but

building up the additional data structures for the virtual three-dimensional element layers used in the 2D flow/3D thermal analysis. Careful attention is however needed for the nodal numbering and elemental connectivity as this impacts the performance and code complexity. The additional thermal nodes and their numbering should preserve the connectivity graph of the original finite element nodal mesh configuration. Two numbering schemes for the thermal nodes (used in serial implementations) and scalable developments are shown in figure 2.

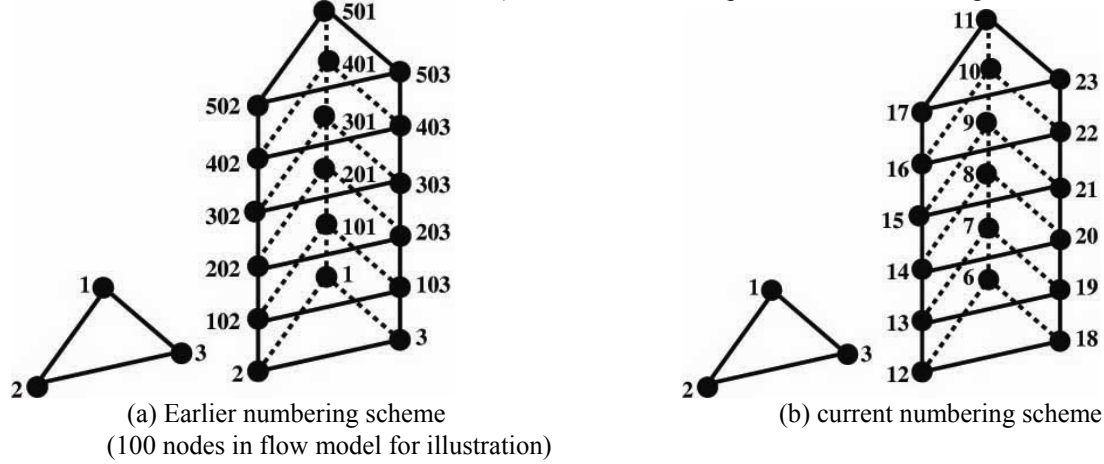


**Figure 2: Stack of Six-Noded Wedge Elements for the 3D Thermal Analysis Built from 2D Flow Thin Shells**

The current numbering scheme shown in figure 2(b) preserves the shape of the nodal connectivity graph. The earlier thermal node numbering algorithm (figure 2(a)) does not preserve the nodal connectivity graph. If a Reverse Cuthill McKee (RCM)<sup>19</sup> pass is performed on the connectivity graph of the resin flow model, this optimization will also be maintained for the present thermal node numbering. Minimization of the connectivity graph bandwidth can lead to improvements in runtime and cache efficiency of the non-isothermal computations.<sup>13, 14</sup> Further discussions of the non-isothermal scalable implementations and developments are presented in references 20, 21 and 22.

The scalable coupled flow-thermal simulations have been ported and tested on several high performance scalable computing architectures. The scalable coupled flow-thermal computations and implementations are validated with available experimental data. The complexity and the multi-physics and transient progression of the problem do not present a potential for any analytical or closed form solutions. Numerical time-temperature history data from coupled flow-thermal simulations are verified and validated against available experimental data. One such validation based on a non-reactive resin stimulant with a viscosity that varies with temperature is presented next. This is followed by the discussions and analysis of scalable non-isothermal computations.

## EXPERIMENTAL VALIDATION

A rectangular mold cavity that is filled with a continuous random glass fiber preform with a fiber volume fraction of 9% as presented by Chiu, et. al.<sup>23</sup>. The experimental mold cavity is of size 21 cm × 7.63 cm × 0.8cm. The mold cavity is injected with a non-reactive liquid system (viscosity changes with temperature) at a constant flow rate from one end. This problem also provides a validation for the scalable non-isothermal computations under flow rate injection conditions that are commonly used in the process. The published experimental details note that the temperature of the mold wall is maintained at 63° C with the liquid system injected at 34.5° C. The temperature dependent viscosity (with the viscosity expressed in Pa-s) of the non-reactive Palatino oil used in the experiment is given by.

$$\mu = 0.001 \exp\left(\frac{4485.2}{T} - 11.3\right) \quad (19)$$

The physical properties for the simulations employed values as provided in the published references.<sup>6, 23</sup> The time-dependent experimental temperatures (time-temperature response) were obtained using thermocouples positioned along the length of the mold cavity and mid-way through the cavity thickness<sup>23</sup>. The time-dependent nodal temperature results at the measured locations (thermocouples located at 0.25L, 0.5L and 0.75L from the inlet and



(20)

$$\hat{S}_p = \frac{p_{min} T_{p_{min}}}{T_p}$$

$p_{min}$  is the smallest number of processors that were used in the computations for a given problem.  $T_p$  is the computational solution time associated with given number of processors.

The test problem used for the performance analysis of scalable non-isothermal computations is a simple risk reduction box geometry shown in figure 4(a). This test case is employed primarily to study the performance of the scalable computations and the analysis capabilities of the physics based finite element modeling and scalable non-isothermal computations for general complex built-up geometries. The finite element model for the non-isothermal computations employed 14,715 nodes and 29,144 triangular elements for the 2.5D thin shell flow domain. This corresponds to 88,290 nodes and 145,720 six-node wedge elements for the full three-dimensional thermal/cure model. The physical properties are taken to be same as the common properties in the field. The temporal resin infusion progression from the scalable non-isothermal computations is shown in figure 4(b). The temperature profile near to the completion of resin infusion is shown in figure 4(c). The scalable computation results are physically consistent. The complete run time for the scalable thermal computations were obtained in three different high performance computing architectures (SGI Origin 3900, IBM P-Series 690 and Linux Networx Evolocivity cluster) in conjunction with computational scientists at Army Research Laboratory. The scalable computations utilized 8, 16, 32, 64 and 128 processors of these machines using nodal based domain decomposition of the problem domain into the same number sub-domains as the number of processors used for the scalable computations.

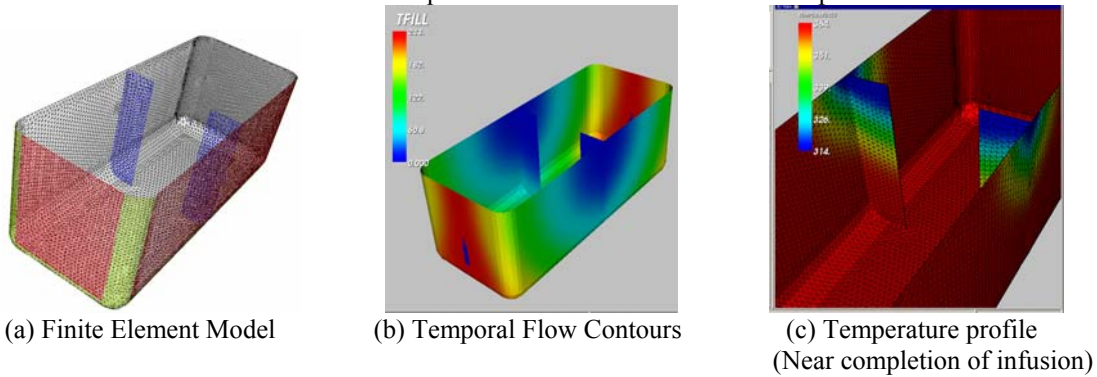


**Figure 4: Demonstrative Coupled Flow-Thermal Scalable Process Modeling Simulations**

The relative speed up of the scalable non-isothermal computations for this problem is shown in figure 5. A careful analysis of the relative speed-up shown in figure 5 indicates that the relative speed-up is super-linear in all the computational runs on different number of processors. A sub-linear relative speed-up is observed only the case of IBM P-690 for 64 processors. An analysis of the computations indicate that majority of the computational time is spent in the application of the thermal boundary conditions to each of the thermal nodes corresponding to the unfilled (fill factor < 1) nodes in the flow problem domain. The computational time in this thermal boundary condition application involves nested loops over the number of nodes. The computational cost involved in the application of the thermal conditions from this nested loop is a cubic function of number of nodes as given by

$$f(n) = \sum_{i=1}^n cn(n-i) = cn^3 - \left( \frac{n^3 + n^2}{2} \right) \quad (21)$$

The computing cost is of order  $n^3$ . This bound also holds for the multi-processor runs. The thermal boundary conditions are applied over the unfilled nodes assigned to a given processor partition based on nodal domain decomposition. For a fixed problem size used in these computations for the relative speed-up, as the number of processors (CPUs) employed increases, the number of nodes assigned per processor (CPU) decreases linearly  $\{O(n)\}$ . The computational load however decreases non-linearly  $\{O(n^3)\}$ . This is reflected in the reduced clock time for the computations with increased number of processors and is potentially causing the super-linear speed-up seen in this case.

The performance of the scalable computations is also influenced by the high performance computing architecture. For example, the performance in IBM-P690 shows a sudden drop in performance from 32 to 64 processors. This machine is based on heterogeneous memory architecture with shared memory within the computing nodes inside a SMP (shared memory processor) box and distributed memory outside each of the SMP boxes. Each SMP box of larger systems consist 32 processors. The SMP nature of the IBM system while within the box and distributed memory while going outside the box could account for the sudden drop in performance when going from 32 to 64 processors.

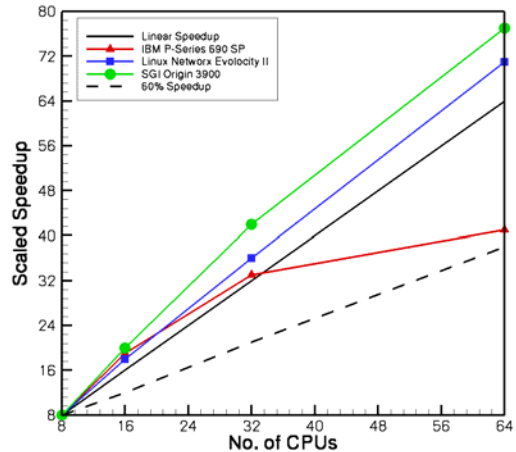


**Figure 5: Scalable Performance of Coupled Flow-Thermal Simulations (Demonstrative Problem in Figure 4)**

## CONCLUDING REMARKS

This paper focused and addressed the computational issues in the coupled flow-thermal scalable process modeling and simulations for the manufacture of polymer composite structures via net shape manufacturing processes such as the resin transfer molding. The coupled flow-thermal transport phenomena that exist in the liquid composite molding processes require effective numerical approaches and techniques for the analysis of the multi-physics phenomena. An effective implicit pure finite element methodology for the solution of the transient moving front in Eulerian mesh geometries is coupled with stabilized Petrov-Galerkin approaches to computationally model the coupled thermal transport that exists and governs the process. The physical and computational complexity of the manufacturing process and composite structural configurations manufactured requires the use of high performance computing resources and robust techniques for scalable software developments. Computational issues in the scalable implementations for the coupled flow-thermal phenomena are briefly highlighted. An illustrative experimental validation of the coupled flow-thermal scalable developments is also presented. Scalable performance results and analysis of the coupled flow-thermal developments from three different computing architectures is also presented. The present developments have evolved into validated and robust scalable simulation analysis software for the coupled flow-thermal process modeling of thin-shell composite structural configurations by resin transfer molding.

## ACKNOWLEDGEMENTS

The author acknowledges the collaborations and contributions of D. Shires, B. Henz, N. Ngo, K. Tamma, and others. The author acknowledges the support from U. S. Army Research Laboratory, ARO-Battelle Scientific Services Program, and Department of Defense High Performance Computing Modernization Program.

## REFERENCES

1. R.V. Mohan, et al, *Polymer Engineering and Science*, **39**(1), 26 (1999).
2. M.V. Brusckke, S.G. Advani, *Polymer Composites*, **11**(6), 398, (1990).
3. F. Troughu, R. Gauvin, D. M. Gao, *Advances in Polymer Technology*, **12**(4), 329, (1992).

4. L. J. Lee, et al, Composite Structures, **27**, 109 (1994).
5. V. M. Gonzalez, Ph.D. Thesis, University of Minnesota, (1983).
6. N. Ngo, Ph.D. Thesis, University of Minnesota, (2001).
7. R. B. Dassenberger and C. L. Tucker, Polymer Composites, **16**(6), 495, (1995).
8. T.J.R. Hughes, et al, Computer Methods in Applied Mechanics and Engineering, **59**, 85, (1986).
9. A. N. Brooks and T. J. R. Hughes, Computer Methods in Applied Mechanics and Engineering, **32**, 199, (1982).
10. S. Balay, et al, PETSc Users Manual, Argonne National Laboratory, (2001).
11. M. Joshi, et al, PSPACES: Scalable Parallel Direct Solver Library for Sparse Symmetric Positive Definite Linear Systems, Department of Computer Science, University of Minnesota, (1999).
12. R. V. Mohan, D. R. Shires, and A. Mark, Scalable Large Scale Process Modeling and Simulations in Liquid Composite Molding, In Proceedings of the 2001 International Conference on Computational Science, Springer-Verlag Lecture Notes in Computer Science, San Francisco, May 2001.
13. D. Shires and R. Mohan, J. Mathematical Modeling and Algorithms, **1**, 153, (2002).
14. D. Shires and R. Mohan, J. Supercomputing, **25**, 131, (2003).
15. R.V. Mohan, et al, J. Advances in Engineering Software, **29** (3-6), 249, (1998).
16. D. R. Shires and B. J. Henz, An Object-Oriented Approach for Parallel Finite Element Analysis, In *International Conference on Parallel and Distributed Processing Techniques and Applications*, Las Vegas, NV, June 2003.
17. G. Karypis, V. Kumar, METIS: A Software Package for Partitioned Unstructured Graphs and Partitioning Meshes, Univ. of Minnesota.
18. G. Karypis, V. Kumar, ParMETIS: A Software Package for Partitioned Unstructured Graphs and Partitioning Meshes, Univ. of Minnesota.
19. E. Cuthill and J. McKee, Reducing the Bandwidth of Sparse Symmetric Matrices, In Proceedings of the 24<sup>th</sup> National Conference, 157, Association of Computing Machinery, (1969).
20. R. Mohan, B. Henz and D. Shires, Coupled Scalable Multi-Physics Simulations for Liquid Composite Molding Processes: Recent Developments and Computational Performance, 11<sup>th</sup> International Conference on Composites/Nano Engineering, Hilton Head, 2004.
21. B. Henz, D. Shires, R. Mohan, A Parallel Computational Environment for Modeling the Resin Transfer Molding Process, 8<sup>th</sup> International Conference on Numerical Methods in Industrial Forming Processes, 2004.
22. B. Henz, D. Shires, R. Mohan, Development and Integration of Parallel Multidisciplinary Computational Software for Modeling a Modern Manufacturing Process, 6<sup>th</sup> International Meeting on High Performance Computing for Computational Science, June 2004.
23. H. T. Chiu, et al, Analysis of Heat Transfer and Resin Reaction in Liquid Composite Molding, ANTEC 97, 2424-2429, (1997).